IEEE Access
Multidisciplinary | Rapid Review | Open Access Journal

Received 18 November 2022, accepted 30 November 2022, date of publication 26 December 2022,
date of current version 6 January 2023.

*Digital Object Identifier 10.1109/ACCESS.2022.3232294*

RESEARCH ARTICLE

# Revamped Sine Cosine Algorithm Centered Optimization of System Stabilizers and Oscillation Dampers for Wind Penetrated Power System

**S. GRACE SADHANA, (Member, IEEE), S. KUMARAVEL, (Senior Member, IEEE), AND S. ASHOK, (Senior Member, IEEE)**

Department of Electrical Engineering, National Institute of Technology at Calicut, Calicut, Kerala 673601, India

Corresponding author: S. Kumaravel (kumaravel_s@nitc.ac.in)

This work was supported by the Project "GaN-Based High Gain DC/DC Converter Fed Multi-level Inverter for UPS Application," through NaMPET-III under Grant 25(12)/2019-ESDA.

**ABSTRACT** The mapping of damping ratios and damping factors by Sine-Cosine Algorithm (SCA) is significant in the analysis of low frequency oscillations generated in an integrated network having multiple conventional and renewable energy sources. Multiple random models with unknown search spaces and uncertain conditions and constraints, which incorporate the fluctuation of solutions towards or outwards at the initial stage for solving real-time problems can be analyzed by a revamped sine-cosine algorithm (RSCA) model. In this paper, the SCA has been revamped to explore the stability threshold for a stable system under dynamic nonlinear operating conditions. It is achieved with the infusion of suitable mathematical functions for optimizing the parameters of Power System Stabilizers (PSSs) and Doubly Fed Induction Generator (DFIG) system-based oscillation dampers to enhance the Small Signal Stability of power systems through effective damping of low-frequency oscillations (LFOs). These LFOs weaken the effective power generation and demand management cycle in conventional power systems when the system faces conditions like intermittent renewable energy sources, overloading conditions, impulsive faults etc. The small-signal and transient stability studies for various disturbances and different operating conditions are investigated, and the performance of the proposed RSCA for optimized parameter tuning of system stabilizers and oscillation dampers are analyzed on the modified benchmarking systems with wind generators using MATLAB® simulations. The efficiency and robustness of the proposed algorithm has been verified under selective critical operating conditions, line outages, and load uncertainties to prove that the low frequency modes are damped with an elevated positive damping ratio and rapid settling time with reduced oscillations. The application of system stabilizers and oscillation dampers optimized through the proposed RSCA shows a reduced settling time in the LFOs created and improved damping ratio of 0.22 for an increase in 20% loading and 50% of wind power generation in the case study of Two Area Four Machine System.

**INDEX TERMS** Low-frequency oscillations, optimization problem, power system stabilizer (PSSs), power oscillation dampers (PODs), sine-cosine algorithm, wind energy conversion systems (WECS).

## I. INTRODUCTION

### A. BACKGROUND AND CHALLENGES

Power system security necessitates the integration of remotely located Renewable Energy Sources (RESs) into the power grid. Among all RESs, wind turbines have the potential in meeting the demand of 20 times greater than the requirements of a given population [1], [2]. Integrating RESs is fraught with numerous challenges; power system instability, varying generating and loading conditions, unpredictable changes in network structures due to fault, and the intermittent nature of RESs. These challenges result

The associate editor coordinating the review of this manuscript and approving it for publication was Nagesh Prabhu.

in small-signal instability conditions by generating Low-Frequency Oscillations (LFOs) having frequencies ranging from 0.1 Hz – 2.0 Hz [3].

### B. LITERATURE REVIEW

The power transfer capability between areas in conventional power systems reduces as there is a sustained increase in the LFOs. The increase in rotor angle deviation of synchronous machines due to sustained LFOs results in a loss in synchronism and eventually leads to small signal instability if sufficient damping torque is not produced. The LFOs are of two types, the local mode of oscillations with a frequency range of 0.8 Hz to 2 Hz and the inter-area mode of oscillations with frequency range from 0.2 Hz to 0.8 Hz [4]. The suitable control structure for providing sufficient damping torque in the form of voltage signals in tandem with the Automatic Voltage Regulator (AVR) and generator excitation system is Power System Stabiliser (PSS) based control architecture. The performance and resilience of PSS for enhancing the stability margin of power systems is upgraded by several control based techniques, in which Fuzzy Logic based Power System Stabiliser (FLPSS) design for damping electro-mechanical modes of oscillations have been presented in [5]. In comparison with a multi-zonal PID (Proportional-Integral-Derivative) controller structure, Conventional Power System Stabiliser (CPSS) and FLPSS, confirm that a rule-based FLPSS provides a higher stability margin under several conditions [6]. Other control techniques, such as H$\infty$ [7], Neural Network (NN) [8], and Sliding Mode Control (SMC) [9] have been suggested for the optimal design of PSS. In these methods, the control law depends on a linearized machine model, and the control parameters are adapted under certain nominal operating conditions. However, tuning of PSS parameters independent of other systems' parameters has been found to be insufficient when the Wind Energy Conversion System (WECS) is integrated with conventional energy sources in the power grids [10].

### C. MOTIVATION

The wind generation system mainly utilizes Doubly Fed Induction Generators (DFIGs) to control both active and reactive power and can transfer the output power at various wind speeds [11]. The important aspects of DFIG can be summarised as the provisioning of good damping to the weak area of the power grid, decreasing the damping of the inter-area oscillatory mode, and reducing the damping when there is an increment of wind power to the system [12]. The addition of an auxiliary damping control loop with a Low Inertia system is mainly provided to handle the stress on power systems and manage the weak ties from collapsing while integrating WECS and thereby enhancing the damping of LFOs. The Power Oscillation Dampers (PODs) are like PSSs, which are installed with either the Rotor Side Converter (RSC) control block or Grid Side Converter (GSC) control block of DFIGs for handling the power oscillations generated in the system due to uncertainties in wind penetration [13]. The inputs of control parameters can be defined as, a change in speed of the wind generator, active and reactive power change, and change in terminal voltage.

The equipment of WECS with PODs affects the LFOs and damps the oscillations eventually. However, the cascaded integration of control loops of the same structure intervenes the adaptability of initially tuned parameters of PSSs which eventually results in inefficient damping of LFOs [14]. This issue of lack of coordination among the control loops in a multi-machine system can be resolved by introducing multi-objective meta-heuristic optimization-based techniques. Thus, a systematic approach to coordinate and design probabilistically Robust wide-area PSS and POD for suppressing inter-area oscillations in wind-connected systems has been performed using the firefly algorithm [15]. The results prove that damping of oscillations has been more effective when there is a coordinated control between the PSSs and PODs than making them operate separately. Further improvement of stability of the system by optimizing the PSS and POD gain using bio-inspired algorithms [16], crowding genetic algorithms with a new objective function named Root Mean Square Deviation (RMSD) [17] has been suggested. The results from the literature have shown that the stabilizing effect of PSS without coordinated control is lower than that of the tuned PSS and DFIG equipped with POD [18].

### D. CONTRIBUTIONS

This paper proposes a novel multi-objective parameter optimization technique viz. Revamped Sine Cosine Algorithm (RSCA) for coordinated tuning of the parameters of the cascaded control loops PSS-SGs and POD-WECS for damping the LFOs. The RSCA is developed to determine the optimal parameters of PSSs and PODs for improving the stability phenomena in the power system by minimizing the damping factor and maximizing the damping ratio of the swing modes. The proposed RSCA is derived from Sine-Cosine Algorithm (SCA) [19] and developed for solving a real challenging constrained problem with an unknown search space and global optimum [20]. In power systems, SCA has been applied for obtaining optimal power flow solution, and power system stability enhancement on a multi-machine system with PSS and other FACTS devices [21]. In this paper, SCA has been revamped to perform the coordinated tuning of the parameters of the PSSs and PODs for RESs integrated power systems. The effect of faults under different working conditions along the developed RSCA-based coordinated tuned PSSs and PODs performance has been analysed on Kundur Two Area Four Machine System and the results were compared with CPSS and CPOD, WOA based PSS and POD [22].

### E. PAPER ORGANISATION

The paper is organized as follows: Section 2 presents the proposed controller algorithm for optimization. Section 3 gives the description of the system model and the detailed model of wind generation and controllers. The simulation study and

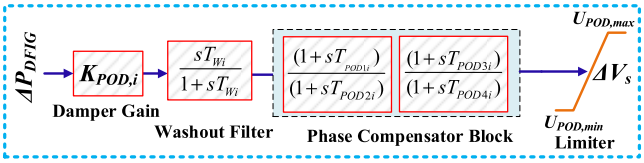


**FIGURE 1.** Block diagram of POD.

the discussion of results are given in Section 4. The paper is concluded in Section 5.

## II. PROPOSED ALGORITHM FOR THE COORDINATED TUNING OF PSSs AND PODs

The integration of wind generation with conventional power systems demands for an effective damping. This is achieved with the help of an auxiliary PSS loop, i.e., PODs connected with the wind generation system [23]. This auxiliary control loop helps in preventing the RES integrated power systems from the additional low frequency oscillations generated by wind generation based systems. The proposed optimization algorithm co-ordinately tunes the parameters of the PSSs and PODs and improves damping by operating the PSSs connected to the SGs and PODs connected to the wind that creates the LFOs. The SCA is an iterative swarm intelligence strategy-based optimization algorithm that generates the random solution through global search thread for large disturbances and local search threads for weak and small disturbances [19]. This is performed through the trigonometric sine cosine functions. The implementation of linear search space and addition of empirical parameter in the traditional SCA for obtaining stable solutions through global search space makes the proposed RSCA suitable for the coordinated parameter optimization of PSSs and PODs. The versatile features of RSCA is employed in solving this parameter optimization problem of a highly complex power systems network when integrated with dynamic RES.

### A. NEED FOR POD

To damp out the oscillations created by the high penetration of wind generation; it is highly essential to develop a control strategy like that of being used in SGs. The effectiveness and robustness of POD mainly depends on the input signal selected for operation. It is always suitable to have a local signal for better damping performance. The POD takes DFIG stator electric power as its measured input signal so that the phase compensation requirement of POD is made simple [24]. The generalized structure of POD is shown in Fig. 1, and the structure is like that of PSS, i.e., a practical second order lead-lag compensator. It consists of a stabilizer gain block $K_{POD,i}$, a washout filter with time constant $T_w$, and a pair of phase compensation blocks with respective time constants $T_{POD1,i}$, $T_{POD2,i}$, $T_{POD3,i}$ and $T_{POD4,i}$. The term 'change in wind power' acts as an input to the POD. The output of the POD is a control parameter. A limiter with minimum and maximum values, were used in the output side of the POD to make a constant output beyond the boundary. $K_{POD,i}$ defines the amount of damping needed to be done by POD so that the phase compensator block provides the suitable lead-lag compensation signal corresponding to the output. The effective stabilization of power system oscillations in wind generation integrated power system happens by coordinated control of PSSs and PODs [25].

where, $i$ is gain of the $i^{th}$ POD, Twi is washout time constant of $i^{th}$ POD, $(i = 1, 2, 3 \ldots n)$, and $T_{PODk,i}$ are the time constants of lead-lag block set of the $i^{th}$ POD $(k = 1, 2, 3 \ldots n)$. The closed loop equation for POD is mentioned in (1).

$$\Delta V_{s,pod,i} = \left[K_{POD,i}\left(\frac{sT_{wi}}{1+sT_{wi}}\right)\left(\frac{1+sT_{POD1,i}}{1+sT_{POD2,i}}\right) \times \left(\frac{1+sT_{POD3,i}}{1+sT_{POD4,i}}\right)\right]\Delta P_{DFIG} \quad (1)$$

A proper fitness function is required to perform this coordinated optimized tuning of PSSs and PODs for robust control and the description for the same is given in the following section.

### B. FITNESS FUNCTION FOR THE COORDINATED TUNING OF PSSs AND PODs

To utilize the benefits of the existing optimization technique developed for coordinated tuning of the PSSs and PODs, the main components of the power systems such as generators and excitation system, PSSs and PODs should be modeled appropriately. These models are used to obtain the optimal solutions based on the objective function. This paper proposes a novel population based heuristic method called RSCA to maximize the accuracy in optimization and find the global optimal value of the fitness function. Proposed objective function describes the necessity of a real part of the eigenvalue known as damping factor and damping ratio of corresponding swing modes to minimize the stability problem in the power system as given in (2)-(3). $p^l$ is number of operating points (Swing Modes), $\zeta_{m,n}$ is damping ratio of $m^{th}$ eigenvalue of the $n^{th}$ operating point, $\sigma_{m,n}$ is real part of the $m^{th}$ eigenvalue i.e. the damping factor of the $n^{th}$ operating point.

$$J_1 = Min\left(\sum_{n=1}^{p^l}\sum_{\sigma_{m,n}\geq\sigma_0}\left[\sigma_0 - \max\left(\sigma_{m,n}\right)\right]^2\right) \quad (2)$$

$$J_2 = Min\left(\sum_{n=1}^{pl}\sum_{\zeta_{m,n}\leq\zeta_0}\left[\zeta_0 - \min\left(\zeta_{m,n}\right)\right]^2\right) \quad (3)$$

The multi-objective problems are converted into a single objective problem by assigning distinct parameters to each. In this case, the conditions are imposed simultaneously by combining the defined objective functions in (2) and (3) as,

$$J_{new} = [\alpha J_1 + \beta J_2]$$

$$J_{new} = \left(\alpha\sum_{n=1}^{pl}\sum_{\sigma_{m,n}\geq\sigma_0}\left[\sigma_0 - \max\left(\sigma_{m,n}\right)\right]^2 + \beta\sum_{n=1}^{pl}\sum_{\zeta_{m,n}\leq\zeta_0}\left[\zeta_0 - \min\left(\zeta_{m,n}\right)\right]^2\right) \quad (4)$$

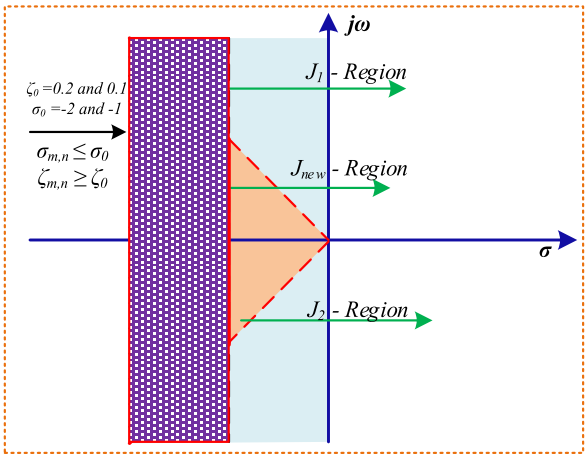


**FIGURE 2.** Desired stable state region of Eigen values.

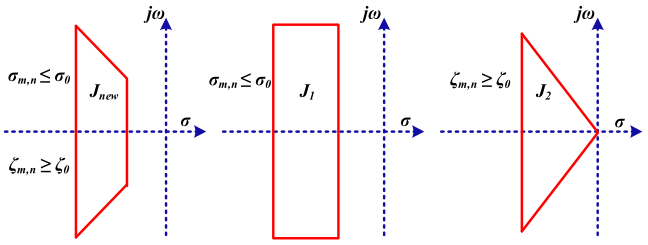


**FIGURE 3.** Desired stable state region of Eigen values separated by Objective functions.

where, $\alpha$ is the randomization parameter, and $\beta$ is the attractiveness parameter. These values are selected after multiple iterations during different conditions. The stability of the power system is enhanced by formulating the constrained optimization problem as given in (4), with the constraints of PSSs and PODs as parameter limits:

$$Min\ J_{new}$$

Subject to the constraints,

$$\begin{aligned}
K_{pss,i,min} &\le K_{pss,i} \le K_{pss,i,max} \\
K_{pod,i,min} &\le K_{pod,i} \le K_{pod,i,max} \\
T_{1i,min} &\le T_{1i} \le T_{1i,max} \\
T_{1i,min} &\le T_{1i} \le T_{1i,max} \\
T_{2i,min} &\le T_{2i} \le T_{2i,max} \\
T_{2i,min} &\le T_{2i} \le T_{2i,max} \\
T_{3i,min} &\le T_{3i} \le T_{3i,max} \\
T_{3i,min} &\le T_{3i} \le T_{3i,max} \\
T_{4i,min} &\le T_{4i} \le T_{4i,max} \\
T_{4i,min} &\le T_{4i} \le T_{4i,max}
\end{aligned}$$

where, $\{i = 1, 2, 3 \ldots n\}$, $n$ is the sum of PSSs and PODs connected in the system. Optimal solution of (4) aids in bringing the system closed-loop eigenvalues in the D-shaped sector in which $\sigma_{m,n} \le \sigma_0$, $\sigma_{m,n} \le \sigma_0$ and $\zeta_{m,n} \ge \zeta_0$ as shown in Fig. 2 and in Fig. 3

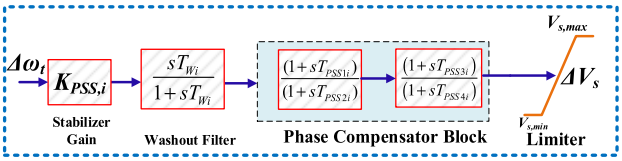


**FIGURE 4.** Block diagram of PSS.

The PSS is mainly added as an auxiliary controller to the AVR of SGs. It aids in reducing as well as damping the LFOs. The input signals can be active power, shaft speed and system frequency and aims at offsetting the phase lag between the excitation system and damping torque component. In the design process of the PSS, the models are linearized around an equilibrium point. The Type-II PSS is considered here for the study and has three state variables. The mathematical equations derived for PSS are given below.

The generalized block diagram of the conventional PSS (CPSS) [26] is shown in Fig. 4, and the closed loop equation is given as, (5)–(8), shown at the bottom of the next page, where, $K_{PSS,i}$ is gain of the $i^{th}$ PSS, $T_{wi}$ is washout time constant of $i^{th}$ PSS, $(i = 1, 2, 3 \ldots n)$, $T_{pss,k,i}$ is time constants of lead-lag block Set of the $i^{th}$ PSS, $(k = 1, 2, 3 \ldots n)$, $\dot{v}_{w,pss,i}$ is the output from washout filter block, $\dot{v}_{c,pss,i}$ is the output from the lead-lag compensator, $\Delta V_{s,pss,i}$ is the output signal of the $i^{th}$ PSS and $\Delta\omega_t$ is the speed deviation of the synchronous machine. To obtain the optimal design of the $i^{th}$ PSS to mitigate the rotor oscillations in an effectual way, the stabilizer gains $K_{PSS,i}$, and the time constants of lead-lag block $T_{PSS,k,i}$ need to be optimized. The simultaneous optimized tuning of PSSs and PODs with respect to a complex network uncertainty is performed by revamping the sine and cosine functions of SCA. The algorithms i) Bio-Inspired Whale Optimization Algorithm ii) Revamped Sine-Cosine Algorithm that are used for the optimization of PSS and POD are presented below.

### C. BIO-INSPIRED WHALE OPTIMIZATION ALGORITHM FOR OPTIMIZING THE PARAMETERS OF PSS AND POD

The Bio-inspired WOA was initially developed by observing the hunting strategy of Humpback Whales in the sea [22]. The Humpback whales follow a technique called bubble net feeding method, while attacking the prey. For reaching the prey, the whale follows two step mechanism, i.e. Shrinking encircle mechanism and Spiral Mechanism. The whole process revolves around a specific single Eigenvalue based objective function with the design parameters. The optimization function defines the thumb rule for the two phases in optimization algorithm, the Exploration phase for getting the Global best solution and Exploitation phase to check for the local best solution. These two phases decide the convergence level of the optimal solutions. The convergence levels of the optimal solutions depend on the balance between the two phases on reaching the solution. This is highly intervened by

the chaotic and stochastic nature of the complex uncertain network.

The steps involved in WOA are as follows,

Step 1: Initialization (No. of Iterations, Population Size, Maximum and Minimum Limits, Starting Solution point)

Step 2: Realization of Objective Function suitable for the PSS parameter optimization

$$X_{ji}^{0} = X_{j}^{min} + rand\left(X_{j}^{min} - X_{j}^{max}\right) \tag{9}$$

$X_j$ is the control variable with maximum and minimum limits, $j = 1, 2, 3 \ldots..N$, $N$- No. of Control Variables. *rand* – random number varies between [0,1]. $i = 1, 2, 3 \ldots N_P$, $N_P$ Population Size.

Step 3: Updating the path of hunting agents- Shrinking Mechanism

$$\vec{S} = \left|\vec{R}.\vec{P} * (t) - \vec{P}(t)\right| \tag{10}$$

$$\vec{P}\,(t+1) = \vec{P}^{*}\,(t) - \vec{A}.\vec{S} \tag{11}$$

where, $\vec{S}$-Distance between the whale and the Prey, $\vec{R}$ & $\vec{A}$ represents a random value ranging (2,0) are the coefficients given in (12-14), $t$- iteration value, $P^{*}(t)$ denotes the optimum solution obtained at the current iteration value, where $P$ is the position. The distance $\vec{S}$ is an absolute value. $\vec{r}$ gives an arbitrary value.

$$\vec{A} = 2\vec{a}.\vec{r} - \vec{a} \tag{12}$$

$$\vec{R} = 2.\vec{r} \tag{13}$$

$$\vec{S} = \left|\vec{R}.\vec{P}_{rand} - \vec{P}\right| \tag{14}$$

$$\vec{P}\,(t+1) = \vec{P}_{rand} - \vec{A}.\vec{S} \tag{15}$$

Step 4: Updating the path of hunting agents- Spiral Mechanism

$$\vec{P}\,(t+1) = \vec{S}' e^{bl}.\cos(2\pi l) + \vec{P}^{*}\,(t) \tag{16}$$

where,

$$\vec{S} = \left|\vec{P}^{*}\,(t) - \vec{P}(t)\right| \tag{17}$$

$$\vec{P}\,(t+1) = \begin{cases} \vec{P}^{*}\,(t) - \vec{A}.\vec{S}, & if\ \delta < 0.5 \\ \vec{S}' e^{bl}.\cos(2\pi l) + \vec{P}^{*}\,(t), & if\ \delta \geq 0.5 \end{cases} \tag{18}$$

where, $\delta$ is the arbitrary value [0,1]

Step 5: Arrival of best solution for PSS parameters.

### D. REVAMPED SINE-COSINE ALGORITHM

The Sine-Cosine Algorithm (SCA) was initially developed using the trigonometric mathematical functions of Sine and Cosine to fluctuate towards and outwards the desired solution [19]. This is a novel population base search algorithm that includes the search phases like WOA, Exploration phase and Exploitation phase for various random and adaptive variables. This algorithm is initially applied to a real time challenging case study, the optimization of cross-section of an aircraft's wing and demonstrated the performance of the algorithm with efficient results. The SCA method creates an air foil with a smooth shape and extremely little drag, proving that it may be highly effective in solving real issues with confined and unknown search areas. The tests are conducted to check for the exploration, exploitation, avoidance of local optima and convergence using various cases with unimodal, multimodal, and composite functions. The performance metrics like search history, trajectory, average fitness of solutions, best solution etc., are used to observe the performance of SCA and confirm the performance both qualitatively and quantitatively. This proves that the SCA can explore the search space by avoiding the local optima and converging towards the global optima by exploiting the search space optimally. The Sine-Cosine trigonometric functions are used as position updating equations which are non-linear in nature. This non-linearity condition limits the capacity of searching while adopted for complex problems. The search path often settles with local best value which declines the quality of the output generated.

The RSCA incorporates an improved position updating equation and improved convergence factor model where the optimization of complex problem with random selection of sine and cosine parameters are retained and the characteristics of dual path, scrubs the absolute value. This in turn enables to have a better convergence factor. With a set of random solutions, the RSCA algorithm begins the optimization process. The algorithm then records the best results thus far, designates it as the goal, and updates all other solutions in relation to it. As the iteration counter increases, the range of sine and cosine functions are modified to highlight exploitation of the search space. When the iteration counter reaches more than the maximum number of iterations, the RSCA algorithm automatically stops the optimization process. Any

$$\dot{v}_{w,pss,i} = -\frac{\left(K_{PSS,i}.\Delta\omega_t + v_{w,pss,i}\right)}{T_{w,i}} \tag{5}$$

$$\dot{v}_{c,pss,i} = \frac{\left(\left(1 - \frac{T_{PSS1,i}}{T_{PSS2,i}}\right)\left(K_{PSS,i}.\Delta\omega_t + v_{w,pss,i}\right) - v_{c,pss,i}\right)}{T_{PSS2,i}} \tag{6}$$

$$\dot{v}_{s,pss,i} = \frac{\left(\left(1 - \frac{T_{PSS3,i}}{T_{PSS4,i}}\right)\left(v_{c,pss,i} + \left(\frac{T_{PSS1,i}}{T_{PSS2,i}}\left(K_{PSS,i}.\Delta\omega_t + v_{w,pss,i}\right)\right)\right) - v_{s,pss,i}\right)}{T_{PSS4,i}} \tag{7}$$

$$\Delta V_{s,pss,i} = \left[K_{PSS,i}\left(\frac{sT_{Wi}}{1+sT_{Wi}}\right)\left(\frac{1+sT_{PSS1i}}{1+sT_{PSS2i}}\right)\left(\frac{1+sT_{PSS3i}}{1+sT_{PSS4i}}\right)\right]\Delta\omega_t \tag{8}$$

additional termination criteria, such as the number of functions evaluated to the maximum or the precision of the global optimum, can be considered. The RSCA outperforms other optimization algorithms since it handles the stochastic nature of the real time problem in an efficient way. The algorithm pictures the optimal tuning problem as a black box and tunes the variables in accordance with the system outputs and constraints. It performs the optimization of the stochastic problems in two phases, (i) exploration and (ii) exploitation phase. The algorithm finds the promising region of the search space by combining the random solution from the set of solutions in the first phase. The promising search space region obtained during the exploration phase is exploited by utilizing the Sine-Cosine functions to obtain optimized results in the second phase. The Revamped Sine-Cosine equations used for updating the positions are given below. Here, $Y_i^t$ denotes the present solution at $i^{th}$ dimension and $t^{th}$ iteration and $S_i^t$ denotes the position of destination point in the $i^{th}$ dimension

$$Y_i^{t+1} = Y_i^t + r_1 sin\sin(r_2)\left|r_3 S_i^t - Y_i^t\right| \quad (19)$$

$$Y_i^{t+1} = Y_i^t + r_1 cos\cos(r_2)\left|r_3 S_i^t - Y_i^t\right| \quad (20)$$

The multiplication function generates the absolute value. Equations (19) and (20) are combined and is given as a single equation with the limiting values as given below.

$$Y_i^{t+1} = \begin{cases} Y_i^t + r_1 sin\sin(r_2)\left|r_3 S_i^t - Y_i^t\right|, r_4 < 0.5 \\ Y_i^t + r_1 cos\cos(r_2)\left|r_3 S_i^t - Y_i^t\right|, r_4 < 0.5 \end{cases} \quad (21)$$

The four key parameters (random numbers) in RSCA are $r_1$, $r_2$, $r_3$ and $r_4$. The description of these parameters are as follows:

1) The random value $r_1$ gives the region of subsequent location or the direction of the parameter to move. This is in between the destination and solution or external to it. The concept of diversification and intensification are well balanced through the sine and cosine trigonometric functions by assigning the value of $r_1$ using (22). Here $a$ is the random number, $T$ denotes the limit to maximum number of iterations and $t$ denotes the number of recent running iteration.

$$r_1 = a - t\left(\frac{a}{T}\right) \quad (22)$$

2) The random variable, $r_2$ calculates distance taken either to move towards the destination or move away from the destination.
3) The arbitrary weight for the destination is assigned through random variable $r_3$ so that the effect of destination in defining the distance is either emphasized or deemphasized.
4) The task of shuffling the values between the sine and cosine functions is done by random variable, $r_4$.
5) The flow chart of the RSCA is shown in Fig. 5. This algorithm is initiated for optimization with a set of random solutions. Then, it saves the best solutions obtained as far as the destination points and updates other solutions based on the best ones. The values of sine and cosine functions are updated for exploiting the search space since updating the iterations. The algorithm is terminated once iteration goes higher than the selected fixed number of iterations. Finally, the best-optimized solution is stored in the destination point and is declared as the global optimum point. The pseudo code for the proposed algorithm followed by the procedure for running stability studies is given below.

ALGORITHM RSCA

**Input:**

1. Set the lower and upper boundary values of $Y$ solutions of $K_{PSS,i}$, $K_{POD,i}$, $T_{pss,k,i,}$ $\{i=1,2,3,4\}$, $T_{POD,k,i,}$ $\{1,2,3,4\}$, where $i=\{1,2,3\ldots,n\}$, $n$= No. of generators. (SGs and wind generators)
2. Set the Population Size of $N$
3. Initialize the parameters with random values.
4. Specify maximum iterations to be $T$
5. Compute the fitness function for the Eigenvalue based multi objective function in (4).

**Output:**

6. The best solutions of $Y^*$ selected for PSSs and PODs

***Loop Process***

1. ***While*** ($t \leq$ Max Iterations $T$) ***do***
2. Calculate fitness function error and convergence.
3. Define the best solution selected ($Y^*$)
4. Update the values of $r_1$, $r_2$, $r_3$ and $r_4$
5. Update the locations in the search space
6. ***end while***
   ***return*** ($Y^*$) for the best solution
7. Preserve the best solution for the objective function with best fitness value.

**Output for Small Signal Stability:**

- Apply the optimized parameters for PSS and POD.
- Run for small signal stability and transient stability conditions with critical uncertain conditions.
- Stable Eigenvalues

This proposed algorithm is validated through simulated case studies, which is provided in the following section.

## III. EVALUATION OF THE PROPOSED METHOD IN POWER SYSTEM STABILITY

### A. STUDY SYSTEM- KUNDUR TWO AREA FOUR MACHINE SYSTEM WITH WIND GENERATORS ALONGSIDE SGs

A standard IEEE Kundur two area four machine power system [27], [28] has been taken to conduct the small signal stability study in this paper. The single line diagram of this power system is shown in Fig. 6 The bus system taken for study is basically segmented into two areas: left half to be area 1 and right half to be area 2. Synchronous machines of 900 MVA and 20 kV are connected in bus 1

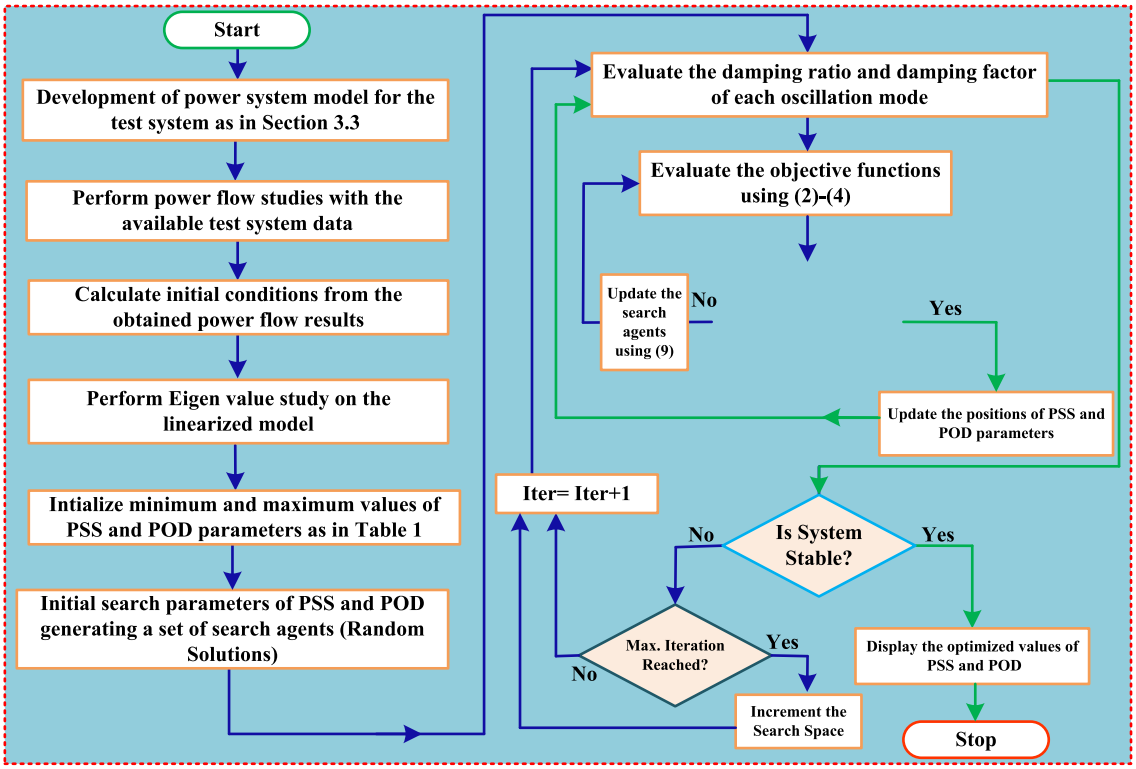


**FIGURE 5.** Flow chart for optimizing the parameters of PSS and POD using RSCA.

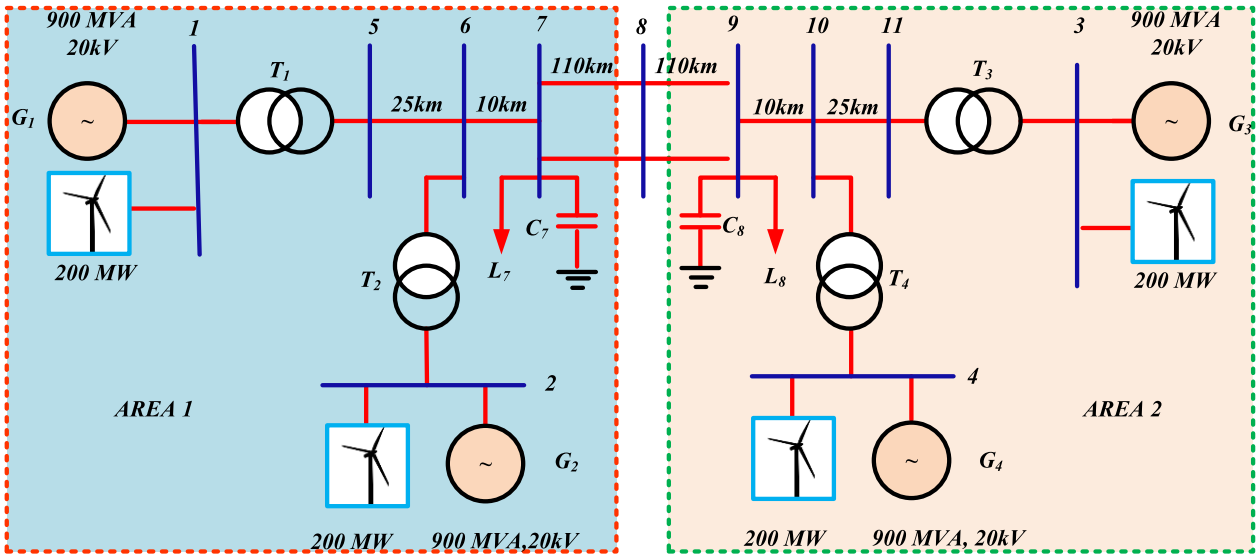


**FIGURE 6.** Single line diagram of kundur two area four machine system with wind generators.

and bus 2 of area 1 and in bus 3 and bus 4 of area 2, and they are represented by a fourth order model equipped with turbine-governor of type II and automatic voltage regulator (AVR) of type III. The system contains eleven buses with a capacity of 230 kV and 20 kV, and two loads connected to bus 7 and bus 9. The two areas are interconnected with a weak tie line located between bus 7 and bus 9. Each synchronous generator in the system taken for study is equipped with PSS and the block diagram of the PSS is given in the following section. Similarly, the DFIGs with a rated capacity of 200 MW are considered, and each is connected at the place where SGs are located. For the analysis,

**TABLE 1. Comparison of optimally tuned parameters of POD and PSS with proposed RSCA.**

| GEN# | ALGORITHM | $K_{PSS}$ | $T_1$ (SEC) | $T_2$ (SEC) | $T_3$ (SEC) | $T_4$ (SEC) |
|---|---|---|---|---|---|---|
| G1 | PROPOSED RSCA | 95.961 | 0.129 | 0.003 | 0.001 | 0.001 |
| | WOA | 1.400 | 0.886 | 0.001 | 0.001 | 0.001 |
| | CPSS | 20 | 0.100 | 0.001 | 0.120 | 0.010 |
| G2 | PROPOSED RSCA | 100 | 0.122 | 0.007 | 0.002 | 0.001 |
| | WOA | 1.411 | 0.001 | 0.003 | 0.001 | 0.001 |
| | CPSS | 20 | 0.100 | 0.001 | 0.120 | 0.010 |
| G3 | PROPOSED RSCA | 3.877 | 0.001 | 0.002 | 0.001 | 0.001 |
| | WOA | 49.860 | 1.417 | 0.001 | 0.001 | 0.001 |
| | CPSS | 15 | 0.100 | 0.001 | 0.120 | 0.010 |
| G4 | PROPOSED RSCA | 69.879 | 0.501 | 0.001 | 0.006 | 0.005 |
| | WOA | 50.814 | 0.884 | 0.001 | 1.811 | 1.705 |
| | CPSS | 15 | 0.100 | 0.001 | 0.120 | 0.010 |
| W1 | PROPOSED RSCA | 2.009 | 0.001 | 0.001 | 0.037 | 0.010 |
| | WOA | 1.410 | 1.132 | 1.652 | 0.001 | 0.001 |
| | CPOD | 10 | 0.318 | 0.192 | 0.318 | 0.192 |
| W2 | PROPOSED RSCA | 66.828 | 0.515 | 0.018 | 0.002 | 66.828 |
| | WOA | 1.411 | 0.001 | 1.999 | 0.001 | 1.404 |
| | CPOD | 10 | 0.318 | 0.192 | 0.318 | 0.192 |
| W3 | PROPOSED RSCA | 22.074 | 0.506 | 0.001 | 0.637 | 0.007 |
| | WOA | 1.410 | 0.001 | 0.0014 | 0.301 | 0.001 |
| | CPOD | 10 | 0.318 | 0.192 | 0.318 | 0.192 |
| W4 | PROPOSED RSCA | 1 | 0.016 | 0.002 | 0.011 | 0.003 |
| | WOA | 1.402 | 0.001 | 1.999 | 0.001 | 0.001 |
| | CPOD | 10 | 0.318 | 0.192 | 0.318 | 0.192 |

each DFIG is equipped with a POD with an aim to damp the LFOs.

The model of Kundur Two Area Four Machine Power System is developed in MATLAB® and PSAT® software to conduct the simulation studies. Initially, the load flow results were obtained for the same and further the modal analysis with the Eigenvalue plot were attained. From the study, the critical Eigenvalues were identified and used for further optimization. The identified critical Eigenvalues are tabulated in Table 3. The coordinated tuning parameters of the PSSs and PODs were done and further the results are depicted by showing the outputs related to change in speed and change in rotor angle of all the generators. The parameters of DFIG considered in this system is given in Appendix.

### B. MATHEMATICAL MODELLING OF SG AND DFIG

The electric power system consists of elements such as generators, transformers, and lines, which are dependent on the size of the system. These interconnections by creating a complex structure, which can generate, distribute, and transmit electricity amongst large areas. Nowadays, the power system models are getting even more complex and very critical to handle due to the addition of RES [29]. The synchronous generator is modelled using $4^{th}$ order model specially to detect and analyze the LFOs and is represented with the set of non-linear differential algebraic equations as given below [30].

$$\dot{\delta}_i = \omega_b \left(\omega_i - 1\right) \tag{23}$$

$$\dot{\omega}_i = \frac{1}{M_i}\left(P_{mi} - P_{ei} - D_i\left(\omega_i - 1\right)\right) \tag{24}$$

$$\dot{E}'_{qi} = \frac{1}{T'_{d0}}\left(E_{fdi} - \left(x_{di} - x'_{di}\right) i_{di} - E'_{qi}\right) \tag{25}$$

$$\dot{E}_{fdi} = \frac{1}{T_{Ai}}\left(K_{Ai}\left(v_{refi} - v_i + u_i\right) - E_{fdi}\right) \tag{26}$$

Here, $\dot{\delta}_i$ gives the rotor angle deviation of SGs, $(n_g \times 1)$, $n_g$ - no. of SGs

$\dot{\omega}_i$ gives the rotor speed deviation of SGs, $(n_g \times 1)$

$\dot{E}'_{qi}$ & $\dot{E}_{fdi}$ gives the q-axis, d-axis transient internal and field voltage deviation, $(n_g \times 1)$.

The above equations are given by considering $i^{th}$ machine in the power system, where, $E_{fdi}, E'_{qi}$, are field and internal voltages, $i_{di}, i_{qi}$ are *d-axis* and *q-axis* armature current, and $x_{qi}, x'_{di}$, are *q-axis* & *d-axis* transient reactance of generator.

The dynamic equations for Type III AVR and Turbine Generator and Governor model are given below, (27)–(30), as shown at the bottom of the next page. Here, $\dot{V}_{m,i}$ gives the measured voltage deviation in AVR, $(n_g \times 1)$

$\dot{V}_{r,i}$ gives the Regulated voltage deviation in AVR, $(n_g \times 1)$

$\dot{V}_{f,i}$ gives the field voltage deviation in AVR, $(n_g \times 1)$

$\dot{X}_{g,i}$ gives the Signal Deviation in the governor, $(n_g \times 1)$.

The DFIG based variable speed wind generation system is one of the RESs considered for case study in this paper. Power is fed through both the stator and rotor windings in this type of generator. A power converter is employed in the rotor circuit to process the slip power. The use of this type of converter is to allow bidirectional power flow in the rotor circuit so that the speed range of the generator is increased. This type of system feature improves the overall power conversion efficiency by performing Maximum Power Point Tracking (MPPT). DFIG can extract maximum amount of energy even at lower wind speeds by finding the optimal speed of the turbine [31]. The maximum power production is directly proportional to the wind speed. There are certain assumptions made during the modelling of the DFIG and are mentioned below.

1) Synchronous reference frame is adopted for developing the dynamic relations.
2) The direct axis lags the quadrature axis by 90°.

The stator of the induction machine is provided with three phase windings, which produce the rotating magnetic field. This rotating field rotates at a synchronous speed. A set of equations were derived for expressing the stator and rotor voltages in the *d-q* axis synchronously rotating reference frame. Flux linkage equations were also derived according to the voltage and current laws. The complete model for the DFIG was obtained by combining the equations describing the voltage and current values of the machine including the swing equation, which provides rotor speed as one of the state variables [32]. The voltage equations with respect to the direct and quadrature axis of stator and rotor are expressed as given below.

$$V_{ds} = R_s I_{ds} - \omega_s \psi_{qs} + \frac{d\psi_{ds}}{dt} \tag{31}$$

$$V_{qs} = R_s I_{qs} + \omega_s \psi_{ds} + \frac{d\psi_{qs}}{dt} \tag{32}$$

$$V_{dr} = R_r I_{dr} - s\omega_s \psi_{qr} + \frac{d\psi_{dr}}{dt} \tag{33}$$

$$V_{qr} = R_r I_{qr} + s\omega_s \psi_{dr} + \frac{d\psi_{qr}}{dt} \tag{34}$$

$$s\omega_s = \omega_s - \omega_r \tag{35}$$

The active and reactive power generated by the DFIG are expressed in (36)-(37), that describes the electrical section of the DFIG.

$$P = V_{ds} I_{ds} + V_{qs} I_{qs} + V_{dr} I_{dr} + V_{qr} I_{qr} \tag{36}$$

$$Q = V_{qs} I_{ds} - V_{ds} I_{qs} + V_{qr} I_{dr} - V_{dr} I_{qr} \tag{37}$$

The electro-mechanical torque generated by the DFIG is given below.

$$T_e = \frac{3}{2}\frac{p}{2}\left(\psi_{qm} I_{dr} - \psi_{dm} I_{qr}\right) \tag{38}$$

$$\psi_{qm} = \psi_{qs} - I_{qs} L_{ls} \text{ and } \psi_{dm} = \psi_{ds} - I_{ds} L_{ls} \tag{39}$$

where, the $\psi_{qm}$ and $\psi_{dm}$ are the *q-axis* and *d-axis* air gap flux linkages. The Differential algebraic equations for converter currents [33] as well as the DFIG rotor speed deviation and pitch angle deviation are given below.

$$\dot{\omega}_{wind} = \frac{(T_m - T_e)}{2H_m} \tag{40}$$

$$\dot{\omega}_{rotor} = \frac{(T_{sh} - T_e - D_t \omega_r)}{2H_g} \tag{41}$$

$$\dot{\theta}_{pitch} = \left(\frac{K_p \phi\left(\omega_m - \omega_{ref}\right) - \theta_{pitch}}{T_p}\right) \tag{42}$$

$$\dot{i}_{qr} = \left(\frac{-\left(\frac{x_s + x_m}{x_m . v}\right) p^*_\omega\left(\omega_{gen}\right)}{\omega_{gen} - \dot{i}_{qr}}\right)\frac{1}{T_e} \tag{43}$$

$$\dot{i}_{dr} = \frac{K_v\left(v - v_{ref}\right) - v}{x_m - \dot{i}_{dr}} \tag{44}$$

Here, $\dot{\omega}_{wind}$ gives the wind speed deviation, $(l_w \times 1)$,

$l_w$ – No. of DFIGs

$\dot{\omega}_{rotor}$ gives the Rotor Speed Deviation of DFIG, $(l_w \times 1)$

$\dot{\theta}_{pitch}$ gives the Deviation in Pitch Angle, $(l_w \times 1)$

$\dot{i}_{qr}$&$\dot{i}_{dr}$ gives the q-axis and d-axis current deviations in the rotor, $(l_w \times 1)$

$x_m$ and $x_s$ represents the stator and magnetising reactance,

$K_p$&$K_v$ denotes the pitch control gain and voltage control gain,

$T_p$ is the time constant,

$T_m, T_{sh}$&$T_e$ denotes the Mechanical, Shaft & Electrical torque,

$v$&$v_{ref}$ represents the measured and reference voltage,

$\omega_{gen}$&$\omega_{ref}$ represents the generator speed and reference speed,

$\phi$ is the phase compensation,

$D_t$ is the Damping constant,

$H_g$ is the inertia coefficient,

$p^*_\omega(\omega_m)$ is the power-speed characteristics of DFIG system,

$T_p$ represents the time constant of power control.

The parameters of DFIG based wind system are given in Appendix mentioned in Table 5. in detail.

### C. STATE-SPACE MATRIX OF PROPOSED SYSTEM

The DFIG was integrated with the grid through a transmission line and represented using the current injection model. For steady state stability analysis, the linearized model, and the state space equations of the dynamic system with synchronous machines, PSSs, PODs, and RES are expressed as,

$$\dot{\Delta x} = A\Delta x + B\Delta u; \quad \Delta y = C\Delta x + D\Delta u; \ \Delta u = k\Delta y \tag{45}$$

where $x$ is the state variable, $y$ is the output, and u represents the control input signal. The matrices $A$, $B$, $C$ and $D$ are matrices varying to the operating condition. In this power system model, the model of a multi machine network along with the integration of different renewable systems is proposed. The system's matrix size increases for every addition of RES. The dynamic equations of a system with $n$ machines $n_{PSS}$ and $n_{POD}$ are given below. Here the system state matrix is expressed as,

$$[\Delta x] = \big[\Delta\delta_i, \Delta\omega_i, \Delta E_{d_{i'}}, \Delta E_{q_{i'}}, \Delta V_{m_i}, \Delta V_{r_i}, \Delta V_{f_i}, \Delta X_{g_i}, \Delta\omega_{wind}, \Delta\omega_{rotor}, \Delta\theta_{pitch}, \Delta i_{dr}, \Delta i_{qr}, \Delta v_{w,\mathrm{pss},i}, \Delta v_{c,pss,i}, \Delta v_{S,pss,i}, \Delta v_{w,\mathrm{pod},i}, \Delta v_{c,pod,i}, \Delta v_{S,pod,i}\big]^T \quad (46)$$

$[\Delta x]$ = [4 State Variables for each SG, 4 State variables of AVR and Governor, 5 State Variables for each DFIG System, 3 State Variables for each PSS, 3 State Variables for each POD]

$\Delta U_{PSS,i} = \big[\Delta U_{pss1}, \Delta U_{pss2}, \Delta U_{pss3}, \Delta U_{pss4}\big]^T$ gives the control signal from PSSs, $(n_{pss} \times 1)$ and

$\Delta U_{pod,i} = \big[\Delta U_{pod1}, \Delta U_{pod2}, \Delta U_{pod3}, \Delta U_{pod4}\big]^T$ gives the control signal from PODs., $(n_{pod} \times 1)$

$\Delta y$ gives the output vector as Change in Bus Angles and Change in Bus Voltages.

The state-space equation of the system was formed for performing small-signal stability analysis [34]. The combined differential equations after being linearized around a common operating point, and the same is expressed in matrix form as,

$$[\dot{x}0] = [ABDE]\,[xy] + [FG]\,d \quad (47)$$

$$\dot{x} = A_s x + B_s d \quad (48)$$

where, $A_s = A - B(E - ID)$ and $B_s = F - B(E - IG)$. The modal analysis is the effective tool proposed ever since in the study of dynamic stability. This mode shape gives the value of the position of different poles, which further gives the information on the behavior of the system. Using this information, the stability of an unstable system is improved by shifting the power systems Eigenvalues to the left half of the complex plane, which was already at the right half of the complex plane. The mode shape of certain component in the power system gives information about the decay rate and damping ratio of the LFOs found in the machine and other associated system. This information is the key parameter in the proposed scheme because the optimization algorithm purely works based on this parameter. The systems Eigenvalues were obtained by developing solutions for the characteristic equation (49). This equation has the state-space matrix '$A$' with all the elements of power systems confined to it and is denoted by,

$$det(\lambda I - A) = 0 \quad (49)$$

Here $\lambda_i$ gives the solutions for the characteristic equation.

$$\lambda_i = \sigma_i \pm j\xi_i \quad (50)$$

where, $\sigma_i$ is the damping factor and the Damping Ratio ($\zeta_i$) of i$^{th}$ Eigenvalue is calculated using (51)

$$\zeta_i = \frac{-\sigma_i}{\sqrt{\sigma_i^2 + \xi_i^2}} \quad (51)$$

## IV. RESULTS AND DISCUSSIONS

The optimization algorithm proposed is simulated for the system considered using in MATLAB®. To evaluate performance of the coordinately tuned PSSs and PODs, detailed simulation studies for four different cases are conducted. These cases were considered based on the percentage variation in load, change in power penetration from the RES and LLL (three-phase) fault at bus 3 and bus 10 at different times respectively and the same is given in Table. 2.

Through these case studies, the performance of RSCA based coordinated tuned PSSs and PODs (scenario 1) are assessed and compared with the conventional PSSs and PODs and Whale Optimization Algorithm (WOA) tuned PSSs and PODs [22], [35]. From the results, it is inferred that the Modified Kundur system is stable for the base case (Case 1) wherein the system is balanced with no addition of RES. Since, the generations and loads are balanced here, the system remains stable even though multiple 3 $\phi$ faults are initiated at Buses 3 and 10 at the time instant of 1s and 2.5s respectively. The same fault is cleared at 1.5s and 3s respectively.

$$\dot{V}_{m,i} = \left(\frac{V - V_m}{T_r}\right) \quad (27)$$

$$\dot{V}_{r,i} = \left(\frac{\left(K_o\left(1 - \frac{T_2}{T_1}\right)(V_{ref} - V_m) - V_r\right)}{T_2}\right) \quad (28)$$

$$\dot{V}_{f,i} = \left(\frac{\left(\left(V_r + K_o\frac{T_1}{T_2}(V_{ref} - V_m) + V_f^{\circ}\right)\left(1 + S_o\left(\frac{V}{V_o} - 1\right)\right) - V_f\right)}{T_e}\right) \quad (29)$$

$$\dot{X}_{g,i} = \left(\frac{\left(\frac{1}{R}\left(1 - \frac{T_1}{T_2}\right)(\omega_{ref} - \omega) - x_g\right)}{T_2}\right) \quad (30)$$

**TABLE 2.** Case study (base values 100MVA, 60Hz).

| Case No. | System Uncertainties and Disturbances | | |
|---|---|---|---|
| | Load Change | Applied Disturbance | Δω & Δδ ($G_1$, $G_2$, $G_3$, $G_4$) |
| 1 | Base Case (Constant Load with No RES | 3-ϕ fault near bus 3 initiated at 1s and cleared at 1.5s. and fault at bus 10, started at 2.5s and cleared at 3s. | (No Change) System remains stable |
| 2. | Constant Load with 50% RES | 3-ϕ fault at initiated at bus 10 at 2.5s and cleared at 3s | Fig. 7 (a-d), Fig 8 (a-d) |
| 3. | 10% Increase in Loading with 50% RES | 3-ϕ fault near bus 3 initiated at 1s and cleared at 1.5s. and fault at bus 10, started at 2.5s and cleared at 3s. | Fig. 9 (a-d), Fig 10 (a-d) |
| 4. | 20% Increase in Loading with 50% RES | 3-ϕ fault near bus 3 initiated at 1s and cleared at 1.5s. and fault at bus 10, started at 2.5s and cleared at 3s. | Fig 11 (a-d), Fig 12 (a-d) |

Throughout the simulation the system remained stable even though it was disturbed by the faults in between. The response on change in speed of generators and change in load angle are similar for all the three values. The challenging condition is maintained at a perfect balance between the load and the generation and makes the system stable during faults and other uncertainties. To handle this challenging case and to present the potential of the proposed method, case studies 2, and 3 were considered. These cases were handpicked from the various combinations of case studies performed during the research since the significance of the proposed method can be demonstrated effectively. Table 1 shows the evolved parameters of PSSs and PODs with proposed RSCA, WOA and CPSS and Conventional Power Oscillation Dampers (CPOD).

In case study 2, the simulation was performed for the modified Kundur System with 50% of the total wind generation. During this case study, the load of the system was kept constant, and 3-$\phi$ faults at the multiple locations like Bus 3 and Bus 10 were introduced. These faults here represent the uncertainty conditions prevailing in the system. To show the effectiveness of the tuned PSSs and PODs to damp out the oscillations, the change in speed response as well as the change in load angle response were plotted. From the plots, the proposed RSCA coordinated tuned PSSs and PODs showed a quick response to faults in comparison with other methods like WOA and CPSS and CPOD. The settling time and the peak overshoot time were lesser in the proposed coordinated tuned PSSs and PODs in comparison with other two methods. Fig. 7 shows the change in speed for generators 1-4 with respect to the loading conditions and available wind power penetration which is 50%. In this, the responses presented for proposed PSS and POD shows a peak value which is within the permissible limits of stability, shows the rapid action in damping the oscillations. This has also been recorded in the $\Delta\delta$ response presented in Fig.8, the oscillations due to transient instability condition of a three-phase fault at multiple locations are damped at a faster pace when the PSS and POD tuned with other methods showed a sustained oscillation. The overshoot response in the first swing is due to the conditions like adding 50% of wind power penetration to the complex network when it is said to run with a constant load. The undershoot response in the third swing is due to the 3-phase fault introduced (Condition of uncertainty) at Bus 10 around 2.5s. The response shows that the PSS and POD optimized by the proposed RSCA can handle the conditions of uncertainty better than the other two PSS and POD based controls.

Although the proposed RSCA based coordinated tuned PSS and POD has a slight over-shoot for a shorter duration compared to the other two conventional methods, these overshoots are under permissible level, i.e., 0.05 Hz/s to 0.1 Hz/s [36]. Fig. 8 shows the change in load angle value of each generator after applying three phase faults. The results of each method, proposed RSCA, WOA and CPSS and CPOD were compared for all the generators separately as Fig.8 (a-d). In all the generators, a significant oscillation was found even after using the conventional PSSs and PODs and WOA tuned PSSs and PODs.

Case study 3 and 4 had been conducted for 20% increase in loading and for a 3-$\varphi$ fault near bus 3 initiated at 1s and fault at bus 10, started at 2.5s and cleared at 1.5s and 3s respectively. In this case, the total power penetration of RES was still considered to be 50% to bring out the threshold capacity of SGs in handling the load variation along with the faults. The importance of creating multiple three phase faults at different locations and different instants were to observe the effectiveness and efficiency of coordinated tuned PSSs and PODs to damp out the sustaining oscillations. In this case, the WOA tuned PSSs and PODs could not survive the oscillations caused due to multiple events. RSCA based coordinated tuned PSSs and PODs showed a significant response

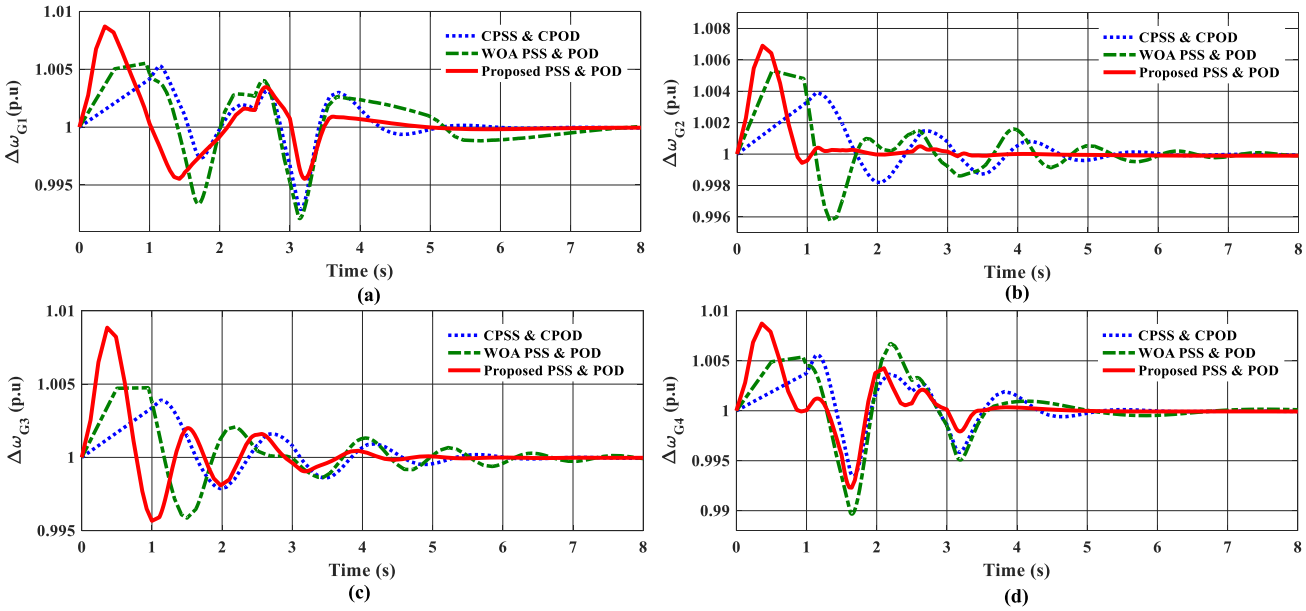


**FIGURE 7.** $\Delta\omega$ response of (a) Generator 1 (b) Generator 2 (c) Generator 3 (d) Generator 4 for constant load and 50% penetration of RES.

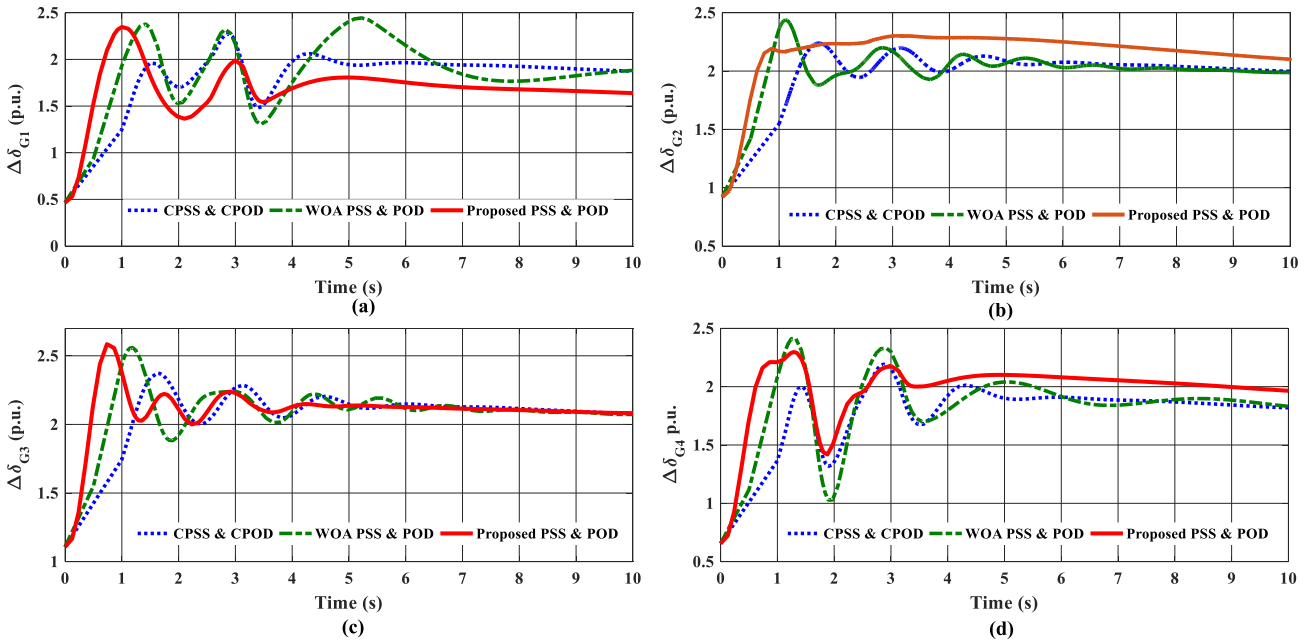


**FIGURE 8.** $\Delta\delta$ response of (a) Generator 1 (b) Generator 2 (c) Generator 3 (d) Generator 4 for 3-$\phi$ fault initiated on Bus 10 at 2.5s and cleared at 3s.

and that is captured as Fig.9-12. This case study aims to assess the performance of the tuned PSSs and PODs in handling uncertainties in the form of multiple faults. Fig.9 (a-d) and Fig.11 (a-d) shows the speed response of each generator while applying the tuned parameters of PSSs and PODs with our three methods. From the figures it was observed that for 10% and 20% increase in loads with only 50% of RES, WOA tuned PSSs and PODs was not able to withstand the fault at multiple locations.

As an effect of this, the system ran into an unstable condition. The corresponding variations with respect to the fault is given in the change in delta plot of each generator under Fig. 12(a-d). For this case where it is complex and critical, proposed RSCA based coordinated tuned PSSs and PODs showed promising results by handing the faults as well as the change in loading conditions. When the fault was created in area 2, the generator 4 located in area 2 oscillated uncontrollably at the initial swing. This sustaining oscillation

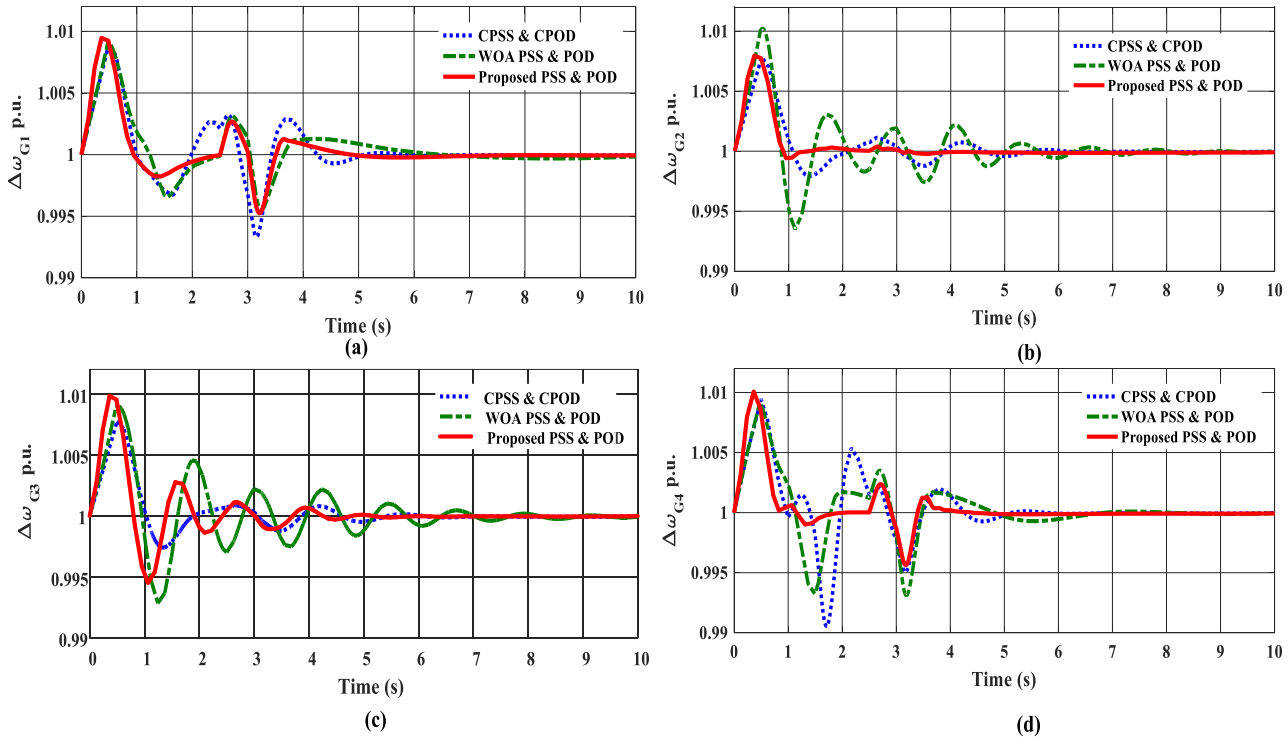


**FIGURE 9.** (a) $\Delta\omega$ response of (a) Generator 1 (b) Generator 2 (c) Generator 3 (d) Generator 4 for 10% Increase in Loading with 50% RES.

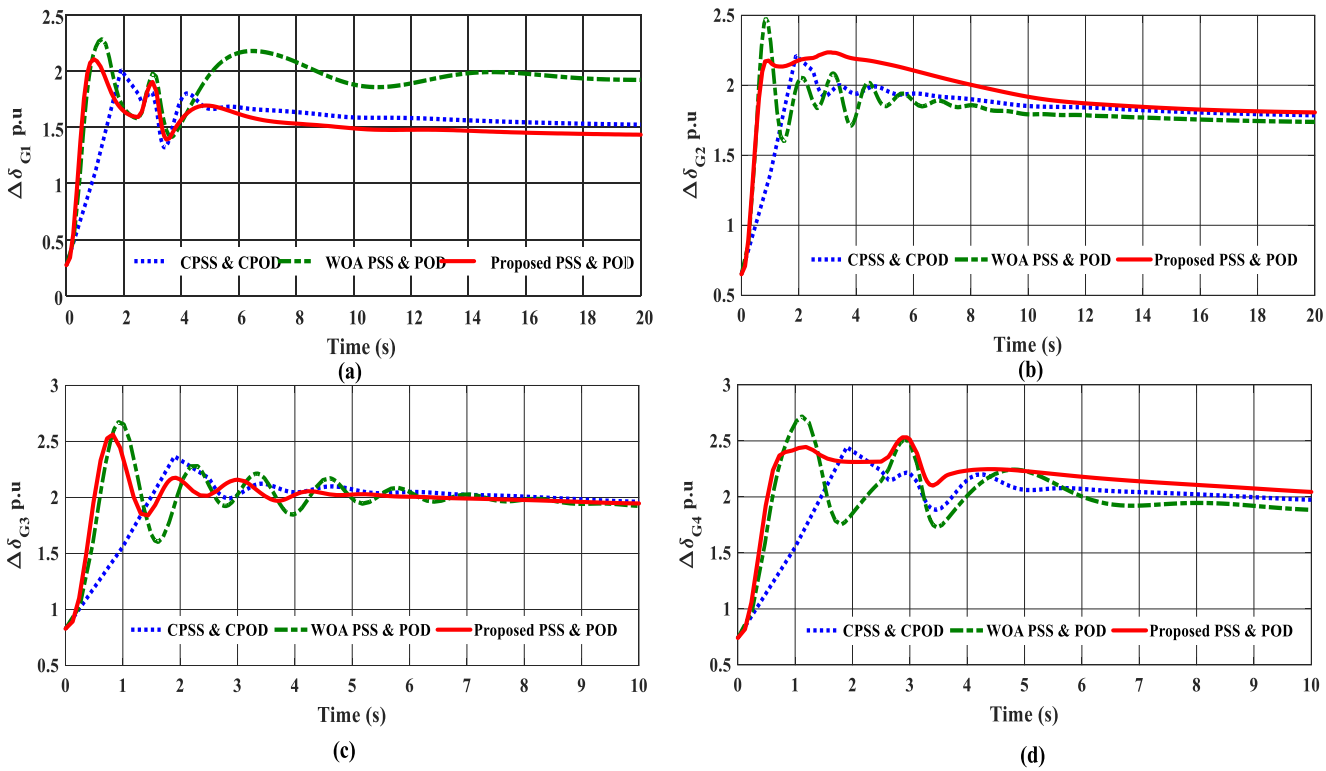


**FIGURE 10.** a) $\Delta\delta$ response of (a) Generator 1 (b) Generator 2 (c) Generator 3 (d) Generator 4 for 3-$\phi$ fault initiated on Bus 3 and 10 at 1s and 2.5s and cleared at 1.5 and 3s.

can grow worse and may lead to loss in synchronism of generator 4.

The worst-case Eigenvalues which have least damping ratio and frequency of oscillation obtained from different case

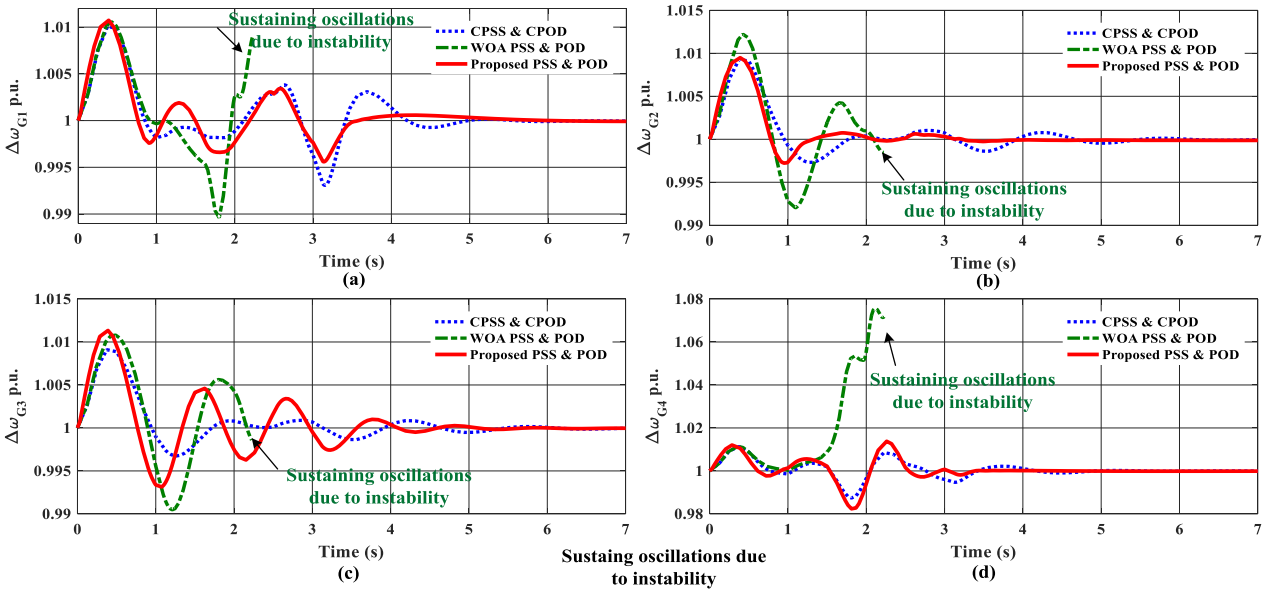


**FIGURE 11.** $\Delta\omega$ response of (a) Generator 1 (b) Generator 2 (c) Generator 3 (d) Generator 4 for 20% increase in loading with 50% RES.

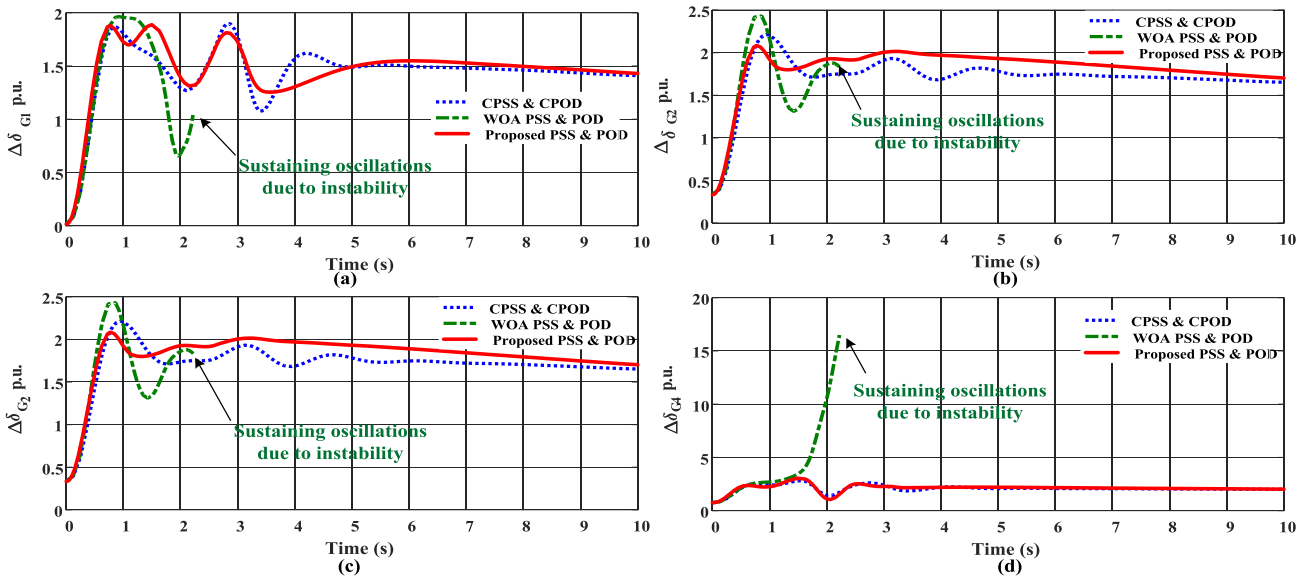


**FIGURE 12.** $\Delta\delta$ response of (a) Generator 1 (b) Generator 2 (c) Generator 3 (d) Generator 4 for 3-$\phi$ fault initiated on Bus 3 and 10 at 1s and 2.5s and cleared at 1.5 and 3sFor scenario.

**TABLE 3.** Critical eigenvalues with damping ratio – two area four machine system.

| SWING MODE | DAMPING RATIO | FREQUENCY (HZ) |
|---|---|---|
| -0.34307±3.5284i | 0.0968 | 0.561 |
| -0.28477±4.7362i | 0.0600 | 0.753 |
| **0.01873± 6.3343i** | **-0.0030** | **1.008** |

**TABLE 4.** Dominant eigenvalue of Case 4.

| | EIGENVALUE (MAX) | DAMPING RATIO | FREQUENCY (HZ) |
|---|---|---|---|
| CPSS&CPOD | 0.018±6.334i | -0.003 | 1.008 |
| WOA PSS & POD | 3.141±22.609i | -0.137 | 3.598 |
| **RSCA PSS & POD** | **-0.180±0.788i** | **0.222** | **0.125** |

studies are displayed in Table 3. For case study 4, the obtained Eigenvalues, damping ratio and frequency respectively are, $0.01873 \pm 6.3343i$, $-0.0030$ and 1.008. Table 3 highlights the improvement in damping ratio for the case of proposed

RSCA based coordinated tuned PSSs and PODs. Compared to the conventional PSSs and PODs, the damping ratio was significantly improved in the proposed RSCA-based coordinated tuned PSSs and PODs as given in Table 4. The presence of a negative damping ratio for the CPSS & CPOD supported power system. This negative damping ratio presents the inefficient damping of CPSS & CPOD when a transient instability condition occurs. The results displayed under $\Delta\delta$ response of generators, the Generator 1 response shows the damping with sustained oscillations whereas the proposed RSCA based PSS & POD can handle the transient instability condition and maintains the system stability. To bring out this significant change in the performance the dominant Eigenvalues are mentioned alongside the display of graphical responses.

## V. CONCLUSION

The idea of revamping SCA for the optimization has been proposed as a novel multi-objective parameter optimization technique viz., Revamped Sine-Cosine Algorithm in the application of coordinated tuning of the parameters of the PSSs and PODs. This improvises the damping ratio and damping frequency of the LFOs generated in a complex power system with high penetration of wind energy generation and thereby maintains the stability. The RSCA utilizes the exploration phase for updating the random target search agent and the exploitation phase for updating the best target search agent in an unknown search space. This makes the algorithm more versatile for real-time problems where the place for uncertain conditions is more with new search spaces. The performance analysis on both the small-signal and transient stability conditions were carried out in Kundur Two Area Four Machine System integrated with WECS alongside the SGs equipped with PSSs and PODs. The proposed coordinately tuned parameters of PSSs and PODs display an improvement in the damping performance for an inter-area LFOs from a poor critical value of $-0.00330$ to 0.222 compared to the CPSS & CPOD and the WOA tuned PSS and POD. Three different cases were considered to experiment the effectiveness of the optimized parameters during uncertainties and sudden faults. The results of transient stability analysis proved that the coordinated tuning of PSSs and PODs was better utilized for an inter-area three-phase fault condition in the system. The proposed method outperforms the other existing methods by bringing the system back into stable mode with damped oscillations for 20 % increase in load with 50% increase in wind power penetration. Whereas the other two methods displayed a result of system going into instability with sustained oscillations and conditions of singularity terminating the performance. The versatility of the proposed algorithm alongside the inclusion of the best location for PSS and POD to improvise the stability of the system is proposed to be done as a future work. In this, the uncertain conditions will be increased even further, and the network adopted will be complex compared to the existing one.

## APPENDIX

**TABLE 5. Parameters of WECS.**

| | |
|---|---|
| Rated Capacity | 200MW |
| Stator Resistance $R_s$ and Reactance $X_s$ | 0.01, 0.10 |
| Rotor Resistance $R_r$ and Reactance $X_r$ | 0.01, 0.08 |
| Magnetization Reactance $X_m$ | 3.00 |
| Inertia Constants $H_g$ | 3 |
| Pitch Control Gain and Time Constant, $K_p$, $T_p$ | 10,3 |
| Voltage Control Gain, $K_v$ | 10 |
| Power Control Time Constant $T_e$ | 0.01 |
| Number of Poles, $P$ and Gear Box Ratio | 4, 1/89 |
| Blade Length, $m$ and number | 75, 3 |
| $P_{max}$ and $P_{min}$ | 1, 0 |
| $Q_{max}$ and $Q_{min}$ | 0.7, -0.7 |

## REFERENCES

[1] National Renewable Energy Laboratory. (Dec. 2008). *20% Wind Energy by 2030 Increasing Wind Energy's Contribution to U.S. Electricity Supply*. [Online]. Available: https://www.nrel.gov/docs/fy09osti/42864.pdf
[2] REN21 Secretariat, Paris, France. *Renewables 2021 Global Status Report*. [Online]. Available: https://www.ren21.net/wpontent/uploads/2019/05/GSR2021_Full_Report.pdf
[3] F. M. Hughes, O. Anaya-Lara, N. Jenkins, and G. Strbac, "A power system stabilizer for DFIG-based wind generation," *IEEE Trans. Power Syst.*, vol. 21, no. 2, pp. 763–772, May 2006, doi: 10.1109/TPWRS.2006.873037.
[4] P. Dey, A. Bhattacharya, and P. Das, "Tuning of power system stabilizer for small signal stability improvement of interconnected power system," *Appl. Comput. Informat.*, vol. 16, nos. 1–2, pp. 3–28, Dec. 2017, doi: 10.1016/j.aci.2017.12.004.
[5] P. Hoang and K. Tomsovic, "Design and analysis of an adaptive fuzzy power system stabilizer," *IEEE Trans. Energy Convers.*, vol. 11, no. 2, pp. 455–461, Jun. 1996, doi: 10.1109/60.507660.
[6] P. K. Ray, S. R. Paital, A. Mohanty, Y. S. E. Foo, A. Krishnan, H. B. Gooi, and G. A. J. Amaratunga, "A hybrid firefly-swarm optimized fractional order interval type-2 fuzzy PID-PSS for transient stability improvement," *IEEE Trans. Ind. Appl.*, vol. 55, no. 6, pp. 6486–6498, Nov./Dec. 2019, doi: 10.1109/TIA.2019.2938473.
[7] Hardiansyah, S. Furuya, and J. Irisawa, "A robust $H_\infty$ power system stabilizer design using reduced-order models," *Electr. Power Energy Syst.*, vol. 28, no. 1, pp. 21–28, Jan. 2006, doi: 10.1016/j.ijepes.2005.09.002.
[8] H. N. Al-Duwaish and Z. M. Al-Hamouz, "A neural network based adaptive sliding mode controller: Application to a power system stabilizer," *Energy Convers. Manage.*, vol. 52, pp. 1533–1538, Feb. 2011, doi: 10.1016/j.enconman.2010.06.060.
[9] S. R. Paital, P. K. Ray, S. R. Mohanty, and A. Mohanty, "An adaptive fractional fuzzy sliding mode controlled PSS for transient stability improvement under different system uncertainties," *IET Smart Grid*, vol. 4, no. 1, pp. 61–75, Feb. 2021, doi: 10.1049/stg2.12002.
[10] N. Gurung, R. Bhattarai, and S. Kamalasadan, "Optimal oscillation damping controller design for large-scale wind integrated power grid," *IEEE Trans. Ind. Appl.*, vol. 56, no. 4, pp. 4225–4235, Jul./Aug. 2020, doi: 10.1109/TIA.2020.2988432.
[11] T. Surinkaew and I. Ngamroo, "Coordinated robust control of DFIG wind turbine and PSS for stabilization of power oscillations considering system uncertainties," *IEEE Trans. Sustain. Energy*, vol. 5, no. 3, pp. 823–833, Jul. 2014, doi: 10.1109/TSTE.2014.2308358.
[12] L. Simon, J. Ravishankar, and K. S. Swarup, "Coordinated reactive power and crow bar control for DFIG-based wind turbines for power oscillation damping," *Wind Eng.*, vol. 43, no. 2, pp. 95–113, Apr. 2019, doi: 10.1177/0309524X18780385.
[13] T. Surinkaew and I. Ngamroo, "Hierarchical co-ordinated wide area and local controls of DFIG wind turbine and PSS for robust power oscillation damping," *IEEE Trans. Sustain. Energy*, vol. 7, no. 3, pp. 943–955, Jul. 2016, doi: 10.1109/TSTE.2015.2508558.

[14] W. C. Wong and C. Y. Chung, "Coordinated damping control design for DFIG-based wind generation considering power output variation," *IEEE Trans. Power Syst.*, vol. 27, no. 4, pp. 1916–1925, Nov. 2012, doi: 10.1109/TPWRS.2012.2190110.
[15] D. Ke and C. Y. Chung, "Design of probabilistically-robust wide-area power system stabilizers to suppress inter-area oscillations of wind integrated power systems," *IEEE Trans. Power Syst.*, vol. 31, no. 6, pp. 4297–4309, Nov. 2016, doi: 10.1109/TPWRS.2016.2514520.
[16] E. L. Miotto, P. B. de Araujo, E. de Vargas Fortes, B. R. Gamino, and L. F. B. Martins, "Coordinated tuning of the parameters of PSS and POD controllers using bioinspired algorithms," *IEEE Trans. Ind. Appl.*, vol. 54, no. 4, pp. 3845–3857, Jul. 2018, doi: 10.1109/TIA.2018.2824249.
[17] P. Lakshmi and K. M. Abdullah, "Stability enhancement of a multimachine power system using fuzzy logic based power system stabilizer tuned through genetic algorithm," *Int. J. Electr. Power Energy Syst.*, vol. 22, no. 2, pp. 137–145, 2000.
[18] X. Y. Bian, Y. Geng, K. L. Lo, Y. Fu, and Q. B. Zhou, "Coordination of PSSs and SVC damping controller to improve probabilistic small-signal stability of power system with wind farm integration," *IEEE Trans. Power Syst.*, vol. 31, no. 3, pp. 2371–2382, May 2016, doi: 10.1109/TPWRS.2015.2458980.
[19] S. Mirjalili, "SCA: A sine cosine algorithm for solving optimization problems," *Knowl.-Based Syst.*, vol. 96, pp. 120–133, Mar. 2016, doi: 10.1016/j.knosys.2015.12.022.
[20] M. Wang and G. Lu, "A modified sine cosine algorithm for solving optimization problems," *IEEE Access*, vol. 9, pp. 27434–27450, 2021, doi: 10.1109/ACCESS.2021.3058128.
[21] M. K. Kar, S. Kumar, A. K. Singh, and S. Panigrahi, "A modified sine cosine algorithm with ensemble search agent updating schemes for small signal stability analysis," *Int. Trans. Electr. Energy Syst.*, vol. 31, no. 11, Nov. 2021, Art. no. e13058, doi: 10.1002/2050-7038.13058.
[22] D. Butti, S. K. Mangipudi, and S. R. Rayapudi, "An improved whale optimization algorithm for the design of multi-machine power system stabilizer," *Int. Trans. Electr. Energy Syst.*, vol. 30, no. 5, May 2020, Art. no. e12314, doi: 10.1002/2050-7038.12314.
[23] J. Zuo, Y. Li, D. Shi, and X. Duan, "Simultaneous robust coordinated damping control of power system stabilizers (PSSs), static var compensator (SVC) and doubly-fed induction generator power oscillation dampers (DFIG PODs) in multimachine power systems," *Energies*, vol. 10, no. 4, p. 565, Apr. 2017, doi: 10.3390/en10040565.
[24] K. Elkington and M. Ghandhari, "Non-linear power oscillation damping controllers for doubly fed induction generators in wind farms," *IET Renew. Power Gener.*, vol. 7, no. 2, pp. 172–179, 2013, doi: 10.1049/iet-rpg.2011.0145.
[25] C. Zhang, D. Ke, Y. Sun, C. Y. Chung, J. Xu, and F. Shen, "Coordinated supplementary damping control of DFIG and PSS to suppress inter-area oscillations with optimally controlled plant dynamics," *IEEE Trans. Sustain. Energy*, vol. 9, no. 2, pp. 780–791, Apr. 2018, doi: 10.1109/TSTE.2017.2761813.
[26] K. R. Padiyar, "Application of power system stabilizer," in *Power System Dynamics: Stability and Control*, vol. 4, 2nd ed. Hyderabad, India: B S Publications, 2008, ch. 8, sec. 8, pp. 264–275.
[27] P. Kundur, "Small signal stability," in *Power System Stability and Control*, vol. 8, 1st ed. New York, NY, USA: McGraw-Hill, 1994, ch. 12, sec. 12, pp. 817–822.
[28] A. A. Alsakati, C. A. Vaithilingam, J. Alnasseir, K. Naidu, and G. Rajendran, "Transient stability enhancement of grid integrated wind energy using particle swarm optimization based multi-band PSS4C," *IEEE Access*, vol. 10, pp. 20860–20874, 2022, doi: 10.1109/ACCESS.2022.3151425.
[29] M. Edrah, K. L. Lo, and O. Anaya-Lara, "Impacts of high penetration of DFIG wind turbines on rotor angle stability of power systems," *IEEE Trans. Sustain. Energy*, vol. 6, no. 3, pp. 759–766, Jul. 2015, doi: 10.1109/TSTE.2015.2412176.
[30] B. M. Alshammari, A. Farah, K. Alqunun, and T. Guesmi, "Robust design of dual-input power system stabilizer using chaotic Jaya algorithm," *Energies*, vol. 14, no. 17, p. 5294, Aug. 2021, doi: 10.3390/en14175294.
[31] P. He, F. Wen, G. Ledwich, and Y. Xue, "An investigation on interarea mode oscillations of interconnected power systems with integrated wind farms," *Int. J. Electr. Power Energy Syst.*, vol. 78, pp. 148–157, Jun. 2016, doi: 10.1016/j.ijepes.2015.11.052.
[32] J. G. Slootweg and W. L. Kling, "The impact of large scale wind power generation on power system oscillations," *Electr. Power Syst. Res.*, vol. 67, no. 1, pp. 9–20, 2003, doi: 10.1016/S0378-7796(03)00089-0.
[33] F. Milano, "Wind power devices," in *Power System Modelling and Scripting*. Ciudad Real, Spain: Univ. of Castilla-La Mancha, 2010, ch. 20, pp. 435–446.
[34] M. A. El-Dabah, M. H. Hassan, S. Kamel, and H. M. Zawbaa, "Robust parameters tuning of different power system stabilizers using a quantum artificial gorilla troops optimizer," *IEEE Access*, vol. 10, pp. 82560–82579, 2022, doi: 10.1109/ACCESS.2022.3195892.
[35] B. Dasu, M. Sivakumar, and R. Srinivasarao, "Interconnected multimachine power system stabilizer design using whale optimization algorithm," *Protection Control Mod. Power Syst.*, vol. 4, no. 1, pp. 1–11, Dec. 2019, doi: 10.1186/s41601-019-0116-6.
[36] J. Zhou, D. Ke, C. Y. Chung, and Y. Sun, "A computationally efficient method to design probabilistically robust wide-area PSSs for damping inter-area oscillations in wind-integrated power systems," *IEEE Trans. Power Syst.*, vol. 33, no. 5, pp. 5692–5703, Sep. 2018, doi: 10.1109/TPWRS.2018.2815534.

**S. GRACE SADHANA** (Member, IEEE) received the B.E. degree in electrical and electronics engineering (EEE) and the M.E. degree in power systems from Anna University, Chennai, in 2011 and 2013, respectively. She is currently pursuing the Ph.D. degree in electrical engineering with the National Institute of Technology at Calicut, Calicut, India. She has more than three years of work experience in academia. Her research interests include power systems stability studies on conventional grids, renewable power integration, and system uncertainty modeling.

**S. KUMARAVEL** (Senior Member, IEEE) received the B.E. degree in electrical and electronics engineering (EEE) from Bharathidasan University, Tiruchirappalli, in 2002, the M.Tech. degree in power systems from the National Institute of Technology (NIT) Tiruchirappalli, in 2007, the Ph.D. degree in electrical engineering from NIT Calicut, India, in 2012, and the P.D.F. degree from University College Dublin, Ireland. Since 2008, he has been an Associate Professor with the Department of Electrical Engineering, NIT Calicut. His research interests include dc-dc converters and microgrid.

**S. ASHOK** (Senior Member, IEEE) received the B.Sc. degree in electrical and electronics engineering (EEE) from the Regional Engineering College, Calicut, India, the M.Tech. degree in energy from the Indian Institute of Technology Delhi, India, and the Ph.D. degree from the Indian Institute of Technology Bombay, India. He is currently working as a Professor with the Department of Electrical Engineering, National Institute of Technology at Calicut. His major research interests include distributed generation, microgrid, deregulation, and power quality.